

Structure and mechanical behaviour of short glass fibre-reinforced ethylene–tetrafluoroethylene copolymers

Part I *Influence of the filler on mechanical behaviour and structure*

E. M. WEIS, W. WILKE

Abteilung für Experimentelle Physik, Universität Ulm, Albert Einstein-Allee 11, D-7900 Ulm, Germany

A copolymer of ethylene, tetrafluoroethylene, hexafluoropropylene and perfluoropropylvinylether has been investigated. Uniaxial tensile tests at small strains showed improved mechanical properties, when the copolymer was filled with short glass fibres. This is due to a change in superstructure, as can be seen with small-angle X-ray scattering (dynamic measurements during heating with synchrotron radiation). This results in some kind of bonding between matrix and fibres: scanning electron micrographs of fracture surfaces obtained at temperatures between -192 and $+160$ °C show the bonding as well as the nucleating influence of the fibres on the matrix in their surroundings. Wide-angle X-ray scattering up to 170 °C (made with a Guinier camera) shows that the crystalline structure itself was not influenced by the fibres and that the crystallites in the copolymer were longitudinally disordered to a high degree.

1. Introduction

Ethylene–tetrafluoroethylene copolymer (ETFE) is a semi-crystalline polymer consisting of mostly alternating monomer units of ethylene (ET) and tetrafluoroethylene (TFE), if the chemical composition of ET:TFE is about 50:50 mol% [1, 2]. This copolymer has some remarkable properties [2]: mechanical behaviour at low and at high temperatures, chemical and thermal resistance and dielectric properties which are comparable to PTFE, and ETFE is also melt-processable.

In this study an ETFE copolymer, containing small amounts of hexafluoropropylene (HFP) and perfluoropropylvinylether (PPVE), was examined. The use of these comonomers makes the material tougher, increases the fracture strain [3] and, therefore, improves machinability. Filling this ETFE-material with short glass fibres leads to improved mechanical properties, as will be seen later, in contrast to the specimens of polyethylene (PE) and polytetrafluoroethylene (PTFE), where filling with the same sort of fibres has no positive influence on the mechanical properties [4].

In order to investigate the structure of the matrix material, the fibre-to-matrix adhesion, and possible changes in matrix structure caused by the fibres, small- and wide-angle X-ray diffraction experiments were carried out and the fracture-surfaces were examined using scanning electron microscopy.

The mechanical behaviour was analysed by making uniaxial tensile tests until failure occurred. Because of a glass transition in the temperature range 80 – 120 °C [2, 3, 5] and the occurrence of a crystal transformation

at about 90 °C [5, 6], observed in the ETFE bipolymer, investigations were carried out at several temperatures up to the melting point of ETFE.

2. Experimental procedure

2.1. Matrix material

The matrix material chosen for this study was an ETFE quaterpolymer consisting of 49.2 mol% ethylene (ET), 47.0 mol% tetrafluoroethylene (TFE), 3.6 mol% hexafluoropropylene (HFP), 0.17 mol% perfluoropropylvinylether (PPVE), with the following characteristics: melting temperature ~ 273 °C, density 1.70 – 1.73 g cm $^{-3}$, and melt flow index (300 °C, load 11 kg) 37 g/10 min (manufacturer's data: Hoechst).

2.2. Fibres

The fibres used were made of an alumina-boro-silicate glass with the following properties [7]: diameter 10 μ m, length 10 – 200 μ m, density 2.53 – 2.55 g cm $^{-3}$. Before the glass fibres were mixed into the matrix material, they were heat-treated at 600 °C to burn off pollution.

Specimens were examined containing 0, 5, 10 and 20 wt% glass fibres (filler content w_f).

2.3. Preparation of the samples

Sheets were pressed between films of polytetrafluoroethylene for 10 min at 295 °C and with a pressure of

0.8 MPa. Those used for the mechanical examinations had a thickness of about 1 mm and those used for the X-ray studies were about 200 μm thick.

2.4. Geometry of the specimen

The specimens used for mechanical testing were cut from the pressed sheets with their form and dimensions as given in Fig. 1.

3. Results

3.1. Uniaxial tensile tests

When an ETFE-specimen is stretched unidirectionally we obtain the stress-strain curve schematically shown in Fig. 2. There the stress, σ , is given by the quotient of applied load, F , which is measured experimentally, and the cross-section, A_0 , of the unstretched specimen

$$\sigma = F/A_0 \quad (1)$$

The deformation ratio, λ , is computed from

$$\lambda = L/L_0 \quad (2)$$

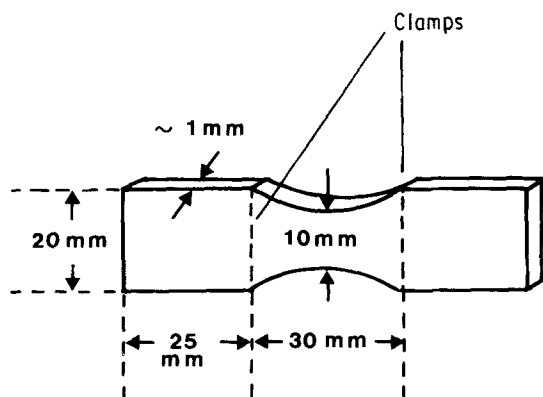


Figure 1 Geometry of the specimen used for mechanical investigations.

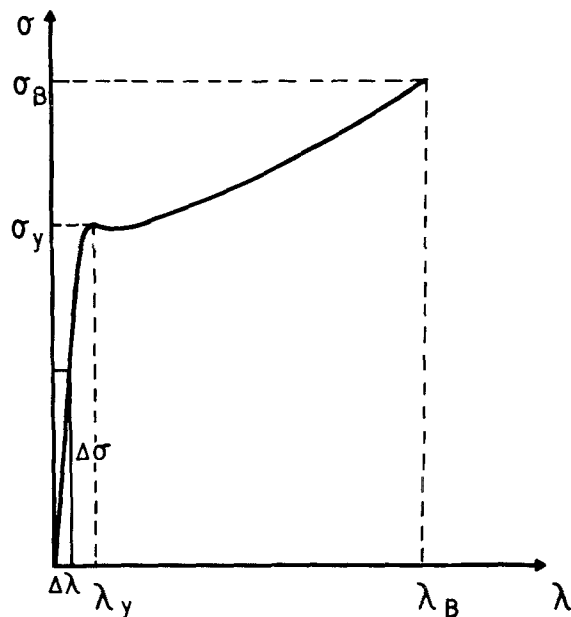


Figure 2 Typical stress-strain curve of ETFE, containing yield point and breaking point.

where L is the actual length and L_0 the original length of the specimen measured between the clamps (see Fig. 1).

For the experiments, four different testing temperatures (-40 , 22 , 80 , 150°C) and a strain rate of $\dot{\lambda} = 2.78 \times 10^{-3} \text{ s}^{-1}$ were chosen.

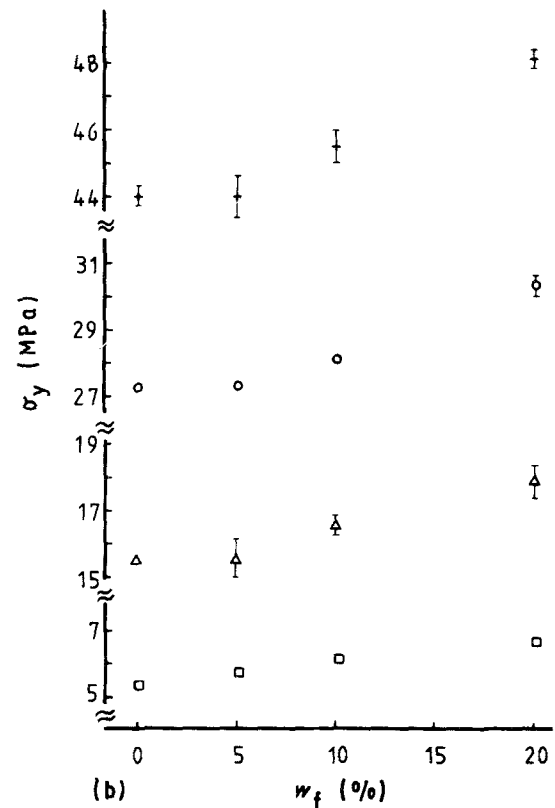
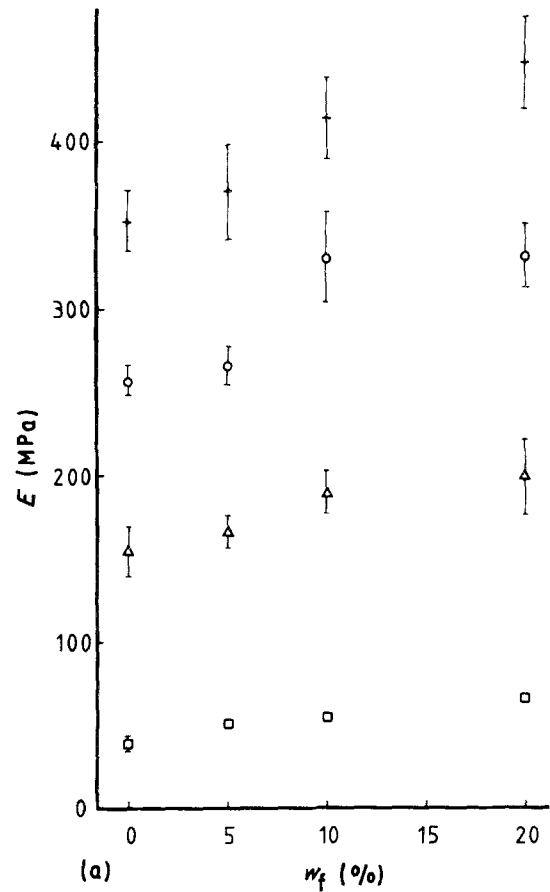


Figure 3a, b

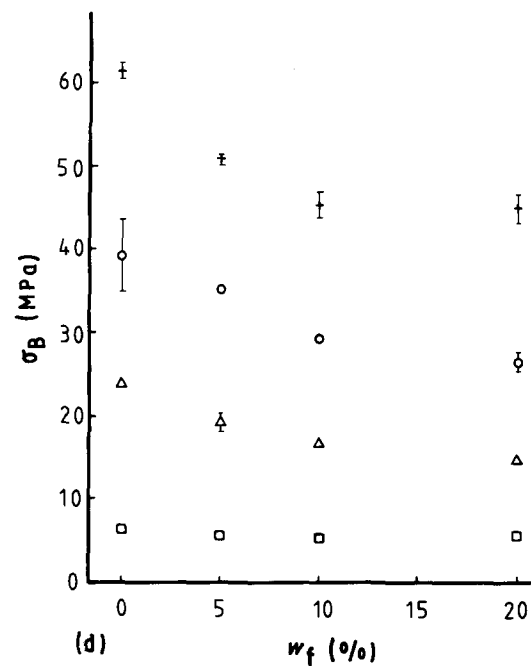
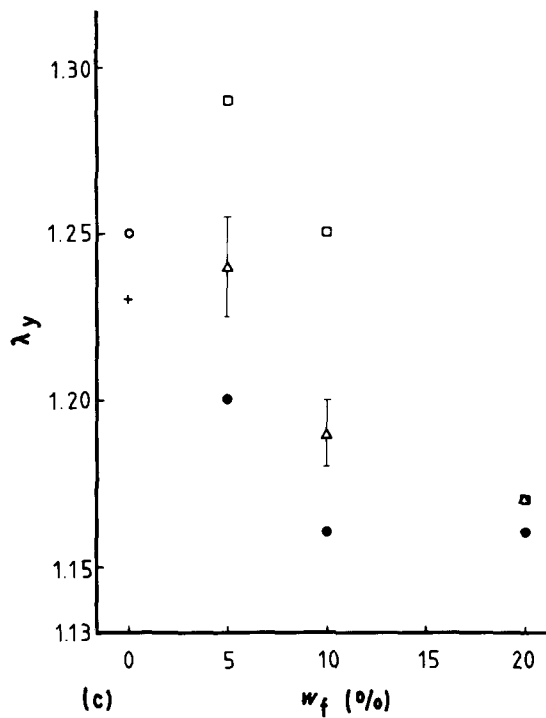
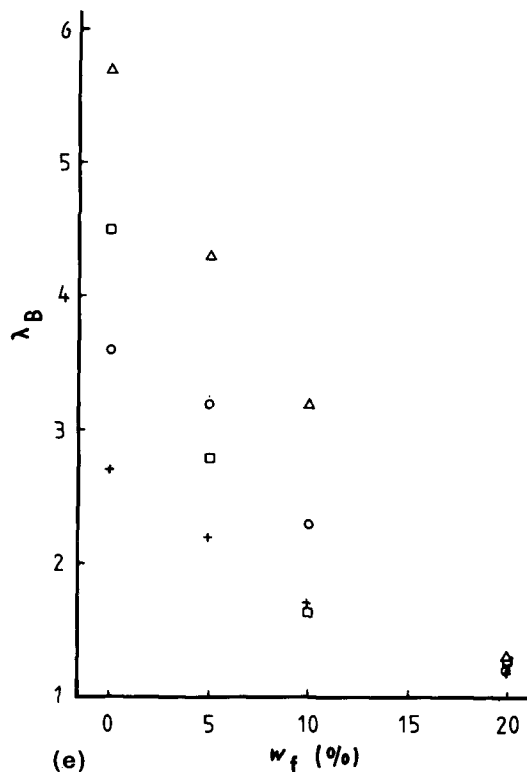


Figure 3 Influence of filler content on (a) E , (b) σ_y , (c) λ_y , (d) σ_B and (e) λ_B ; for several temperatures, T : (+) -40°C ; (O) 22°C ; (Δ) 80°C ; (\square) 150°C .



From the stress-strain curves the following data were obtained:

1. Modulus, E , given as the slope at the origin (note: because of the special geometry of the specimen and the non-static testing conditions, this is not equivalent to the Young's modulus).

2. The deformation ratio, λ_y , and stress, σ_y , at the yield-point.

3. The deformation ratio, λ_B , and stress, σ_B , at the breaking point.

In Fig. 3a-e the changes in these quantities with filler concentration are shown for all testing temperatures. It can be seen that the value of the modulus, E

(Fig. 3a) increases with increasing filler concentration, and decreases with increasing testing-temperature. So, at very small strains, a better stiffness with increasing filler concentration is obtained.

The behaviour at the yield point and (for large deformations) at the breaking-point is interesting when judging the filler influence on mechanical properties. At the yield point, the stress, σ_y , increases (Fig. 3b), although the deformation ratio, λ_y (Fig. 3c), decreases with increasing filler content. With increasing filler content the stress at break, σ_B , approaches a nearly constant value dependent on temperature (Fig. 3d), though the deformation ratio, λ_B (Fig. 3e), strongly decreases.

As expected, the modulus and the measured stresses decrease with higher temperatures.

It is interesting to note that λ_B increases with temperature for temperatures below 100°C and decreases above this. This behaviour has been examined for several ETFE copolymers of different chemical compositions and the temperature where changes in the $\lambda_B(T)$ curve were found to lie between 110 and 120°C [3]. This corresponds to the region where the glass transition is supposed to be. In order to see whether these results could be related directly to the appearance of the obtained fracture surfaces, scanning electron micrographs were taken.

3.2. Scanning electron microscopy

Scanning electron micrographs of failure surfaces obtained by carrying out uniaxial tensile tests at several testing temperatures, T (-100 , 40 , 160°C) are shown in Fig. 4a-c. All the samples had a glass fibre content

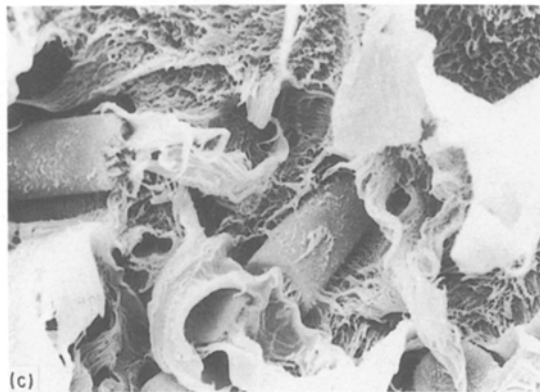
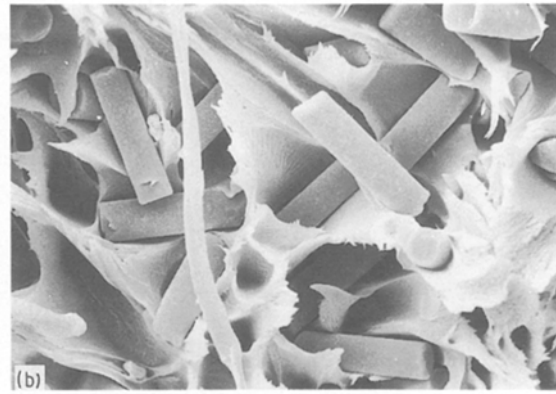
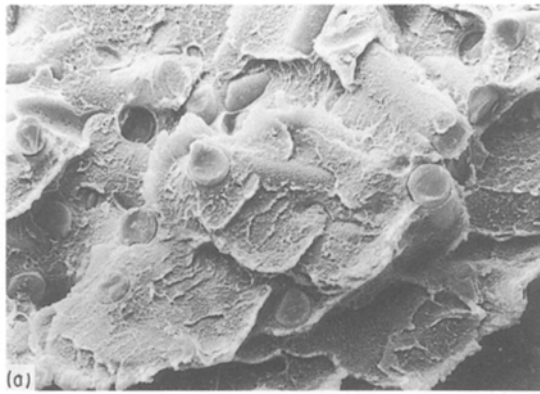


Figure 4 Failure surfaces for different testing temperatures, T (fibre diameter 10 μm): (a) $-100\text{ }^\circ\text{C}$; (b) $40\text{ }^\circ\text{C}$; (c) $160\text{ }^\circ\text{C}$.

of $w_f = 20\text{ wt}\%$. Note that the diameter of the fibres was always 10 μm .

3.2.1. $T = -100\text{ }^\circ\text{C}$ (Fig. 4a)

Obviously failure did not occur at the interface between matrix material and fibre, but occurs rather in the matrix material itself or in the fibres: fibres can be seen covered with matrix material, and there are broken fibres lying perpendicular to the surface. At this testing temperature there was no matrix debonding, due to the brittle failure of the matrix material. The failure of the filled specimens occurs at a deformation ratio of about $\lambda = 1.2$, whilst the unfilled begin to fail at $\lambda \approx 1.8$.

3.2.2. $T = 40\text{ }^\circ\text{C}$ (Fig. 4b)

Here the behaviour is quite different. All fibres are “swimming freely” in the failure surface (none of them are even partially covered with matrix material). In this case failure occurred by matrix debonding because of the toughening of the matrix material at this temperature. Whilst failure of the filled specimen takes place here at a deformation ratio similar to $T = -100\text{ }^\circ\text{C}$ ($\lambda_B \approx 1.3$), the unfilled material fails at large deformations of about $\lambda_B \approx 5$.

3.2.3. $T = 160\text{ }^\circ\text{C}$ (Fig. 4c)

At this temperature filled and unfilled specimens fail at nearly the same deformation ratio, similar to that at the testing temperature of $-100\text{ }^\circ\text{C}$: for the unfilled

material, $\lambda_B \approx 1.3$ and for the filled one $\lambda_B \approx 1.4$ at $160\text{ }^\circ\text{C}$. The material fails in a quite different manner than at $-100\text{ }^\circ\text{C}$. However, there is some bonding between fibres: bridges of matrix material can be seen.

3.3. Small-angle X-ray scattering (SAXS)

To look in more detail at the surroundings of the fibres, we prepared failure surfaces by throwing samples into liquid nitrogen and then quickly breaking them. Fig. 5 shows a scanning electron micrograph taken of this sort of failure surface. Again the filler concentration is 20 wt% and the fibre diameter 10 μm . If we look particularly at fibres perpendicular to the surface, we see that there is a region surrounding the fibres (thickness comparable to the fibre diameter) where the structure is different from that beyond. In order to investigate whether this phenomenon is due to a change in the superstructure of the matrix material caused by the fibres, small-angle X-ray diffraction experiments were carried out.

The SAXS experiments were made using synchrotron radiation (wavelength 0.15 nm) at HASYLAB, DESY, Hamburg. For details of the equipment see [8].

Isotropic specimens filled with 0, 10 and 20 wt% fibres were examined during the heating process (from

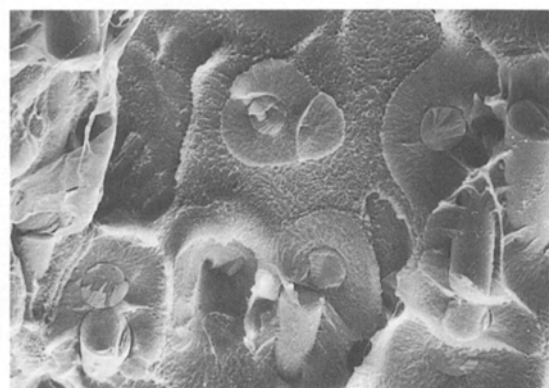


Figure 5 Fibre surroundings in surfaces obtained by breaking at $T = 77\text{ K}$ (fibre diameter 10 μm).

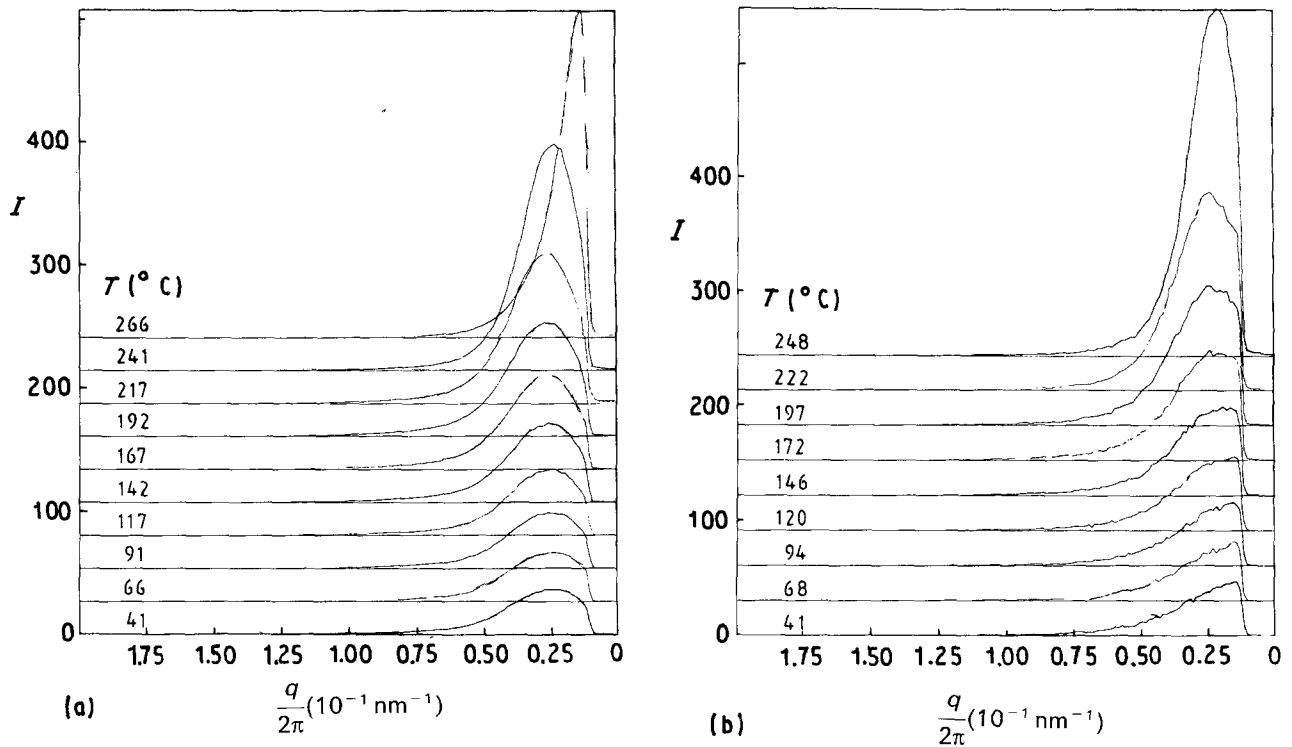


Figure 6 Radial sections of SAXS patterns. (a) $w_f = 0$, (b) $w_f = 20 \text{ wt } \%$.

30–290 °C) (heating rate of 11 K min^{-1}). Radial sections of the diffraction pattern were measured with a position-sensitive detector (PSD) and examples are shown for the case of unfilled and 20 wt % filled specimens in Fig. 6a and b for different temperatures, T . In the case of unfilled ETFE a maximum on the intensity curve is found for all temperatures. The scattering vector, q_{max} , at the maximum was used for the approximate computation of the long period, L , which is a measure of the periodicity in the superstructure (lamellae and fibrils)

$$L = \frac{2\pi}{q_{\text{max}}} \quad (3)$$

$$q = \frac{4\pi \sin \theta}{\lambda} \quad (4)$$

where 2θ is the scattering angle, and λ the X-ray wavelength. The values obtained for the long period are shown in Fig. 7. At low temperatures rather different values are obtained for the long period, depending on the filler content. Approaching the melting point, the difference decreases, and for temperatures above 250 °C the same curve is obtained for all the investigated samples.

Using a vidicon system, the two-dimensional diffraction patterns for stretched samples were also recorded. The samples were not fixed, so they were able to shrink during heating. For deformation ratios smaller than λ_y the above-observed maximum in scattering intensity (anisotropy of diffraction pattern depending on the deformation ratio) was also observed, which first moves away and then approaches the primary beam as the temperature rises. For deformation ratios much greater than λ_y a very intense and anisotropic diffraction pattern was obtained which did

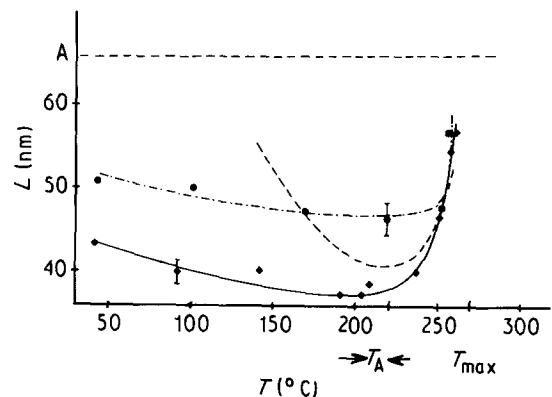


Figure 7 Long period, L , for several filler contents, w_f , depending on temperature, T . w_f : (◆) 0; (●) 10 wt %; (△) 20 wt %. T_A = onset of melting, T_{max} = position of the maximum of the melting peak.

not show a maximum and which is due to micro-voids formed during deformation.

The results of the isotropic samples and the deformation region below the yield point (which yields qualitatively the same) show the influence of the filler on the superstructure of the matrix material. The fibres seem to serve as crystallization nuclei; therefore, greater values for the long period are found for the filled compared with the unfilled material.

3.4. Wide-angle X-ray scattering (WAXS)

The change in superstructure may be accompanied by changes in crystallization parameters such as degree of crystallinity and crystallite size. In order to prove whether these parameters are also influenced by the added filler, line-width measurements of X-ray reflections in the wide-angle region were carried out.

A Guinier camera was used with $\text{CuK}_{\alpha 1}$ radiation to obtain diffraction patterns in the temperature range 20–170 °C. For experimental details see [9]. A typical diffraction pattern of the ETFE material is shown in Fig. 8. One broad reflection can be seen in the observable range, localized at a scattering vector $q = 13.7 \text{ nm}^{-1}$ at room temperature. Because no reflections of higher order appear, the crystallites must be very small and/or badly ordered. WAXS investigations of the crystal structure led to the conclusion that there is only a two-dimensional crystalline order and that in the chain direction the crystals are disordered to a high degree (longitudinal disorder) [10].

For ETFE bipolymers, this reflection is the sum of two overlapping ones for temperatures below 80 °C [5, 10, 11]. Because of a transition at 80 °C from an orthorhombic to a hexagonal crystal structure, these two reflections change to one. For the terpolymer ET/TFE/HFP the same transition has been observed [6].

For a specially treated bipolymer, Tanigami *et al.* [5] obtained a pseudohexagonal structure which produces only one reflection even at temperatures below

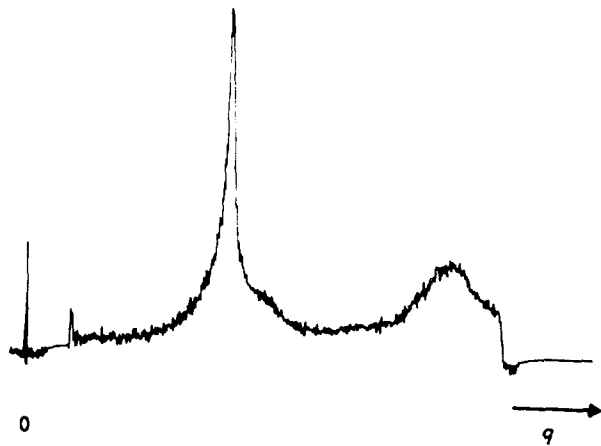
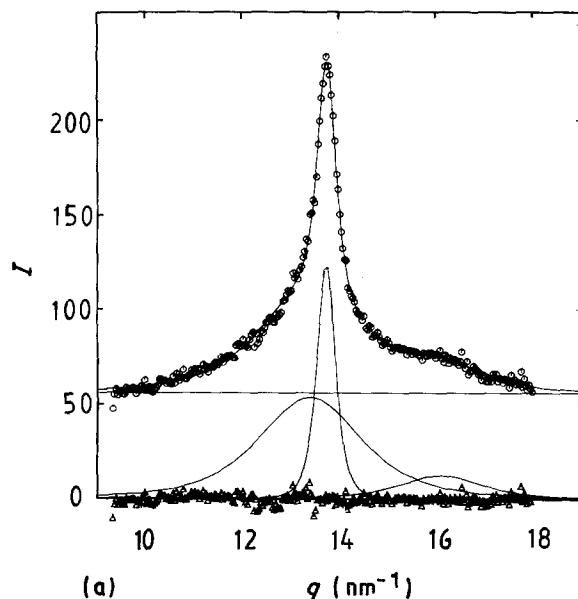


Figure 8 Typical WAXS pattern for ETFE.



80 °C. Lau [12] and Schrodi [3] also found that for the quaterpolymer this reflection is not due to an overlap of two separated reflections. Therefore, it was assumed that the observed reflection was a single one, due to a hexagonal crystal structure.

The digitalized intensity curves of the recorded diffraction patterns were approximated in the range of interest of the scattering vector, q ($9.0 \leq q \leq 18.4 \text{ nm}^{-1}$) with three “squared Lorentz-line”-shaped curves (one for the crystalline reflection and two for the asymmetric amorphous halo)

$$I(q) = I_0 / \left[1 + \left(\frac{q - q_0}{a} \right)^2 \right]^2 \quad (5)$$

and a constant background, with a technique developed by Pieper *et al.* [11]. Examples of these fits are shown in Fig. 9. Near the base line, the difference between the experimental curve and the sum of the four theoretical curves (three Lorentz lines and the background scattering) can be seen. The two lines representing the amorphous scattering are due to one single amorphous phase, because they change position simultaneously with varying temperature.

In Fig. 10 the change in the position of the crystalline reflection, q_c , with temperature, T , is shown. It is interesting that there is no reversible change with temperature. During the heating process the position of q_c remains nearly constant, but on cooling a change occurs. When the temperature increases the small thermal expansion is due to annealing effects, indicating that polymer chains in the crystalline regions are able to gain better order [11]. Therefore, when cooling, initially a higher degree of order exists in the crystallites and the increasing value of q_c is the consequence of thermal contraction.

In Fig. 11 the reciprocal of the integral width of the reflection as a measure of the size of crystalline ordered regions is shown. It is seen that there is no dependence on the filler content, but that for higher

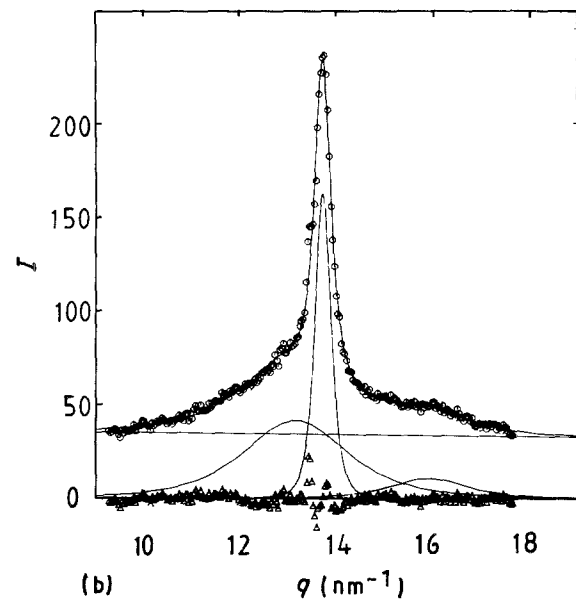


Figure 9 Fits of experimental WAXS data (O) for (a) $T = 40 \text{ °C}$ and (b) $T = 140 \text{ °C}$. (Δ) Difference between experimental data and the sum of all filled lines.

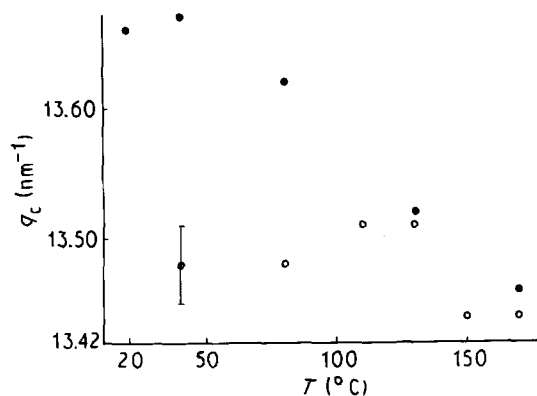


Figure 10 Position of the crystalline reflection, q_c , of the unfilled material: (○) heating; (●) cooling.

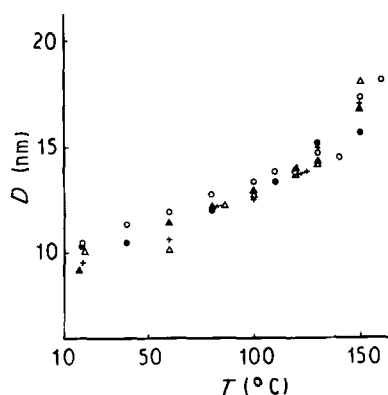


Figure 11 Size, D , of the crystalline ordered regions, depending on temperature, T . $w_f = 0$: (○) heating; (●) cooling. $w_f = 10$ wt%: (△) heating; (▲) cooling. $w_f = 20$ wt%: (+) heating.

temperatures the ordered regions become greater or – more probably, as mentioned above – better ordered. Investigations of the degree of crystallinity showed no influence of the filler concentration.

4. Conclusions

Mechanical properties of ETFE are improved, especially for small strains, by adding short glass fibres. This effect is due to a change in crystallization conditions caused by the fibres. Crystallization was induced in the fibre surroundings (transcrystallinity) which yields a change in superstructure of the matrix material (as can be seen from the SAXS results and the scanning electron micrographs). However, there is no

change in parameters such as crystallite size and crystallinity.

In PE and PTFE, where there are highly ordered crystals, the influence of the fibres seems to be too small to change the crystallization conditions. For ETFE materials, however, this influence is large enough for the glass fibres to act as crystallization nuclei, because of the existence of badly ordered crystalline regions (longitudinal disorder). Thus by adding glass fibres, the mechanical properties of ETFE are improved, whilst those of PE and PTFE are not. Folkes *et al.* [13] obtained a similar effect for polypropylene: transcrystallinity was found in the surroundings of glass fibres only when using adhesion agents.

Acknowledgements

We are grateful for the support of the Bundesministerium für Forschung und Technologie, the Deutsche Forschungsgemeinschaft, Hoechst AG, and we thank the members of the staff of the Polymerbeamline at HASYLAB (DESY Hamburg).

References

1. M. MODENA, C. GARBUGLIO and M. RAGAZZINI, *Polym. Lett.* **10** (1972) 153.
2. C. GARBUGLIO, M. MODENA, M. VALERA and M. RAGAZZINI, *Eur. Polym. J.* **10** (1974) 91.
3. W. T. SCHRODI, Thesis (Diploma), Universität Ulm (1985).
4. J. MAYER, Doctoral Thesis (Dissertation), Universität Ulm (1989).
5. T. TANIGAMI, K. YAMAURA, S. MATSUZAWA, M. ISHIKAWA, K. MIZOGUCHI and K. MIYASAKA, *Polymer* **27** (1986) 1521.
6. S. V. KOSTROMINA, Yu. A. ZUBOV, N. G. SHIRINA and N. F. BAKEEV, *Vysokomol. Soedin. Ser. B* **27** (1985) 620.
7. FA. BAYER, Produktinformation "Glasfaser".
8. G. ELSNER, CHR. RIEKEL and H. G. ZACHMANN, *Adv. Polym. Sci.* **67** (1985) 1.
9. W. WILKE and K. W. MARTIS, *Colloid Polym. Sci.* **252** (1974) 718.
10. K. SCHEERER and W. WILKE, *ibid.* **265** (1987) 206.
11. T. PIEPER, B. HEISE and W. WILKE, *Polymer* **60** (1989) 1768.
12. K. LAU, Thesis (Diploma), Universität Ulm (1984).
13. M. J. FOLKES, P. R. HORNSBY, P. D. SHIPTON and W. K. WONG, in 2nd International Conference, "Short Fibre Reinforced Thermoplastics" (The Plastics and Rubber Institute, 1988).

Received 3 December 1990
and accepted 13 May 1991